

Optomechanical elastomeric engine

Miloš Knežević* and Mark Warner

Cavendish Laboratory, University of Cambridge, Cambridge CB3 0HE, United Kingdom

(Received 24 July 2013; published 24 October 2013)

Nematic elastomers contract along their director when heated or illuminated (in the case of photoelastomers). We present a conceptual design for an elastomer-based engine to extract mechanical work from heat or light. The material parameters and the geometry of such an engine are explored, and it is shown that its efficiency can go up to 20%.

DOI: [10.1103/PhysRevE.88.040501](https://doi.org/10.1103/PhysRevE.88.040501)

PACS number(s): 61.30.-v, 61.41.+e, 83.80.Va, 88.40.-j

Efficiently converting solar energy to mechanical or electrical energy is one of the greatest contemporary challenges in science and technology. In this Rapid Communication we propose an engine based on liquid crystal elastomers (LCEs) [1] that extracts mechanical work from heat or light. As first intimated by de Gennes [2], unusual properties of LCEs arise from a coupling between the liquid crystalline ordering of mesogenic molecules and the elasticity of the underlying polymer network. Various external stimuli, in particular, heat or light, cause reversible contractions of monodomain LCEs along their nematic director, with recovery elongations on stimuli removal. The shape changes of the sample can be remarkable, up to 350%, and occur in a relatively narrow temperature interval around the nematic-isotropic transition temperature [3,4]. The contraction-elongation cycle can be repeated many times, and can be exploited to construct a continuously operating engine in which heat or light is used to produce mechanical work.

Cross-linked networks of polymer chains of an LCE include mesogenic units that belong to either the polymer backbone (main-chain LCE) or side units pendent to the backbone (side-chain LCE) [1]. The shape of a monodomain nematic LCE strongly depends on the temperature-dependent nematic order parameter $Q(T)$, due to the coupling of Q with the average polymer chain anisotropy. Increasing the temperature decreases Q , causing a decrease of the polymer backbone anisotropy, which manifests as a uniaxial contraction of the sample.

A mechanical change of an LCE can also be achieved by introducing photoisomerizable dye molecules into its chemical structure (nematic photoelastomers [5,6]). Upon illumination, dye molecules can undergo transitions from their linear (*trans*) ground state to the excited bent-shaped (*cis*) state. The rodlike *trans* molecules contribute to the overall nematic order, while the bent *cis* molecules act as impurities that reduce the nematic order parameter, in turn leading to a macroscopic contraction.

The operating principle of an LCE engine is shown in Fig. 1. A closed band of a nematic elastomer of initial length L_0 is stretched and wound around two pulleys of radii R_1 and R_2 ($R_2 > R_1$). Initially, the whole elastomeric band is in the nematic state at some temperature T_1 . The transmission pulleys of equal radii r , rigidly coupled with the main wheels, are connected by a loop of inextensible string. Obviously, if

the temperature of the whole system is T_1 , in the absence of external forces, the system is at rest. By increasing the temperature of a part of the elastomer to a value T_2 , an excess contractile force, $f_2 - f_1$, will occur (see Fig. 1). This force acts on wheels of radii R_1 and R_2 and tends to rotate the former counterclockwise and the latter in a clockwise direction; since $R_2 > R_1$ the wheels will turn clockwise. The rotation brings a piece of the elastomer initially being at a temperature T_1 to the temperature T_2 , while another piece of the elastomer having a temperature T_2 returns to the temperature T_1 . By keeping the temperatures T_1 and T_2 at fixed values, this process can be reproduced many times, which provides the basis for a continuous operation of the engine. The engine operation cycle is reminiscent of an engine based on chemomechanical conversion [7]. Our stretch engine is quite different from LCE bend motors [8,9].

Mechanical work can be obtained by applying a suitable external force f_{ext} , for example, by attaching a weight to the end of a thread wound around a pulley of radius r' (see Fig. 1). During the engine operation, a part of the energy invested to heat the elastomer to the temperature T_2 is converted into mechanical work. Another way to realize such an engine is based on the use of photoelastomers. In this case illumination causes the creation of *cis* isomers, which in turn can be seen as a light-dependent increase of the actual temperature T_1 to the new, now effective, value T_2 [5]. Our analysis applies to both thermo- and photoengines.

We shall assume that the elastomer coming in contact with the wheel of radius R_2 changes its temperature from T_1 to T_2 before leaving the wheel, and stays at T_2 until it hits the wheel R_1 . The engine in Fig. 1 requires heating in part AB (illumination in the case of photoelastomers), while in CD cooling to T_1 should be ensured (relaxation to the dark state). Parts BC and DA should be also kept at the constant temperatures T_2 and T_1 , respectively.

In a steady regime, the amount of the elastomer taken on to the wheel of radius R_2 should equal the amount taken on to the wheel of radius R_1 , that is, $\Delta\theta R_2\rho/\lambda_1 = \Delta\theta R_1\rho/\lambda_2$. Here, ρ is the linear density of the elastomer in the formation state at temperature T_1 , $\Delta\theta$ denotes the rotation angle of the wheels, and λ_1 and λ_2 are the stretches in parts DA and BC of the engine, respectively (stretches are measured from the formation state, defined by the initial length L_0 and temperature T_1). We assume that the elastomer in contact with the wheel does not slip, and does not change its length even if it experiences a change of temperature, i.e., the stretch remains

*mk684@cam.ac.uk

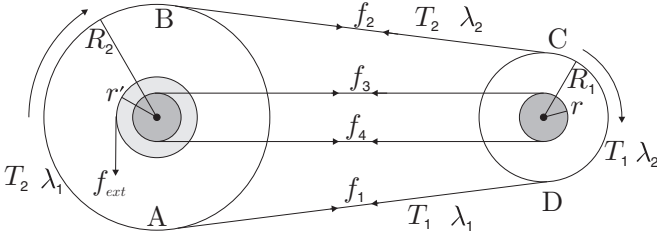


FIG. 1. Schematic of an optomechanical LCE engine.

equal to λ_1 in part AB, and equal to λ_2 in part CD. The above condition can be rewritten as

$$\gamma = \frac{R_2}{R_1} = \frac{\lambda_1}{\lambda_2} \geq 1, \quad (1)$$

where the ratio of the wheel radii is denoted by γ .

To avoid slack, the length L_0 of the elastomer loop in the formation state should be smaller than approximately $2L + \pi(R_1 + R_2)$, where L is the distance BC. Since there is a stretch λ_1 in part DAB of the elastomer and λ_2 in its remaining part BCD, one can write

$$\frac{1}{\lambda_1}(L + \pi R_2) + \frac{1}{\lambda_2}(L + \pi R_1) = L_0. \quad (2)$$

Relations (1) and (2) allow one to express the stretch λ_2 via reduced lengths $\tilde{L} = L/\pi R_1$ and $\tilde{L}_0 = L_0/\pi R_1$,

$$\lambda_2 = \frac{1}{\tilde{L}_0} \left[\tilde{L} \left(1 + \frac{1}{\gamma} \right) + 2 \right]. \quad (3)$$

The inextensible inner wire on the wheels of radii r forces the angular velocities of wheels to be equal (see Fig. 1). When the engine runs at a constant velocity the net torque acting on each of the pulleys is zero. Neglecting frictional forces at the bearings, the balance of torques on wheels of radii R_1 and R_2 is, respectively,

$$\begin{aligned} (f_2 - f_1)R_1 + (f_3 - f_4)r &= 0, \\ (f_1 - f_2)R_2 + (f_4 - f_3)r + f_{\text{ext}}r' &= 0, \end{aligned} \quad (4)$$

where f_3 and f_4 are the forces acting on the wheels of radii r (Fig. 1). From these two equations we get

$$G_{\text{ext}} \equiv f_{\text{ext}}r' = (f_2 - f_1)(R_2 - R_1), \quad (5)$$

where G_{ext} is the magnitude of the torque of the external force f_{ext} . In what follows we express the forces f_1 and f_2 in terms of stretches λ_1 and λ_2 .

Due to the presence of mesogenic molecules, long polymer chains of nematic elastomers have an anisotropic Gaussian distribution. The elastic free energy density of a nematic rubber in response to a deformation λ along the director \underline{n} can be written in the form [1]

$$F = \frac{1}{2} \mu \left(\lambda^2 \frac{\ell_{\parallel}^{(1)}}{\ell_{\parallel}^{(2)}} + \frac{2}{\lambda} \frac{\ell_{\perp}^{(1)}}{\ell_{\perp}^{(2)}} \right), \quad (6)$$

where μ is the shear modulus in the isotropic state. The Flory step lengths in directions parallel and perpendicular to the director \underline{n} have different values ℓ_{\parallel} and ℓ_{\perp} (the director is along the long direction of the elastomeric band). We assume that the elastomer is formed at T_1 (corresponding step lengths are $\ell_{\parallel}^{(1)}$

and $\ell_{\perp}^{(1)}$), and has current step lengths $\ell_{\parallel}^{(2)}$ and $\ell_{\perp}^{(2)}$ (for example, at T_2). Given that we are concerned only with derivatives of F with respect to λ , we omitted λ -independent terms in Eq. (6). As rubber changes shape at a constant volume, the area of the elastomer perpendicular to the director \underline{n} changes by a factor of $1/\lambda$.

The force exerted by an elastomer is proportional to the derivative of free energy density with respect to stretch, $f = A_0(\partial F/\partial \lambda)_T$, where A_0 is the area of the cross section of the elastomer in the formation state. For part DA of the elastomer one has $\lambda = \lambda_1$, $\ell_{\parallel}^{(2)} = \ell_{\parallel}^{(1)}$, and $\ell_{\perp}^{(2)} = \ell_{\perp}^{(1)}$, while for part BC one has $\lambda = \lambda_2$, with $\ell_{\parallel}^{(2)}$ and $\ell_{\perp}^{(2)}$ taking values smaller and larger than $\ell_{\parallel}^{(1)}$ and $\ell_{\perp}^{(1)}$, respectively (for prolate symmetry elastomers). Then the forces f_1 and f_2 are

$$\begin{aligned} f_1 &= \mu(T_1)A_0 \left(\lambda_1 - \frac{1}{\lambda_1^2} \right), \\ f_2 &= \mu(T_2)A_0 \left(\lambda_2 P_{\parallel} - \frac{P_{\perp}}{\lambda_2^2} \right), \end{aligned} \quad (7)$$

where the ratios $P_{\parallel} = \ell_{\parallel}^{(1)}/\ell_{\parallel}^{(2)} > 1$ and $P_{\perp} = \ell_{\perp}^{(1)}/\ell_{\perp}^{(2)} < 1$ depend on the order parameters Q_1 and Q_2 . Note that a free elastomer heated from temperature T_1 to T_2 undergoes the natural contraction $\lambda_m = (P_{\perp}/P_{\parallel})^{1/3}$ along its director (this relation can be obtained by setting $f_2 = 0$ in the above equation).

The isotropic moduli appearing in Eqs. (7) are assumed to be comparable, $\mu(T_1) \approx \mu(T_2)$. On inserting (7) into (5), the reduced torque $\mathcal{G} = (f_2 - f_1)(R_2 - R_1)/\mu A_0 R_1$ is

$$\mathcal{G} = (\gamma - 1) \left[\lambda_2 (P_{\parallel} - \gamma) - \frac{1}{\lambda_2^2} \left(P_{\perp} - \frac{1}{\gamma^2} \right) \right]. \quad (8)$$

We compare this torque to that of the reduced torque $G_{\text{ext}}/\mu A_0 R_1$ from the external forces. Since the ratio γ of the wheel radii is greater than 1, then $\mathcal{G} > 0$ if $[\dots]$ of (8) is positive. We examine four different cases:

(a) $P_{\parallel} - \gamma > 0$ and $P_{\perp} - 1/\gamma^2 > 0$, which is equivalent to $P_{\parallel} > \gamma > 1/\sqrt{P_{\perp}}$, involving a purely material condition $P_{\parallel}\sqrt{P_{\perp}} > 1$. The reduced torque \mathcal{G} as a function of λ_2 is shown in Fig. 2(a) for two different temperatures T_2 and T'_2 ($T'_2 < T_2$). It is easy to see that \mathcal{G} vanishes for $\lambda_2 = [(P_{\perp} - 1/\gamma^2)/(P_{\parallel} - \gamma)]^{1/3}$. At point A the torque \mathcal{G} is greater than the reduced torque of external force $G_{\text{ext}}/\mu A_0 R_1$, and the engine turns more quickly until it does not have time to heat to the temperature T_2 . It only gets to temperature $T'_2 < T_2$ and moves on to the T'_2 curve at point B. This governing of the delivered torque by the speed of rotation is reminiscent of an electric motor; rotation-induced back electromotive force limits current flow and hence limits torque.

(b) $P_{\parallel} - \gamma < 0$ and $P_{\perp} - 1/\gamma^2 < 0$, which can be expressed as $P_{\parallel} < \gamma < 1/\sqrt{P_{\perp}}$, and hence $P_{\parallel}\sqrt{P_{\perp}} < 1$ is the material condition. Now \mathcal{G} is shown in Fig. 2(b), and stability analysis is quite similar to that for case (a).

(c) In the case $P_{\parallel} - \gamma > 0$ and $P_{\perp} - 1/\gamma^2 < 0$, \mathcal{G} is always positive [Fig. 2(c)]. The reduced torque \mathcal{G} has a minimum at $\lambda_2 = [(2(1/\gamma^2 - P_{\perp})/(P_{\parallel} - \gamma))]^{1/3}$, and this minimum decreases by lowering the temperature from T_2 to T'_2 . Again, if one starts at point A where $\mathcal{G} > G_{\text{ext}}/\mu A_0 R_1$, the engine will move to operate at point B.

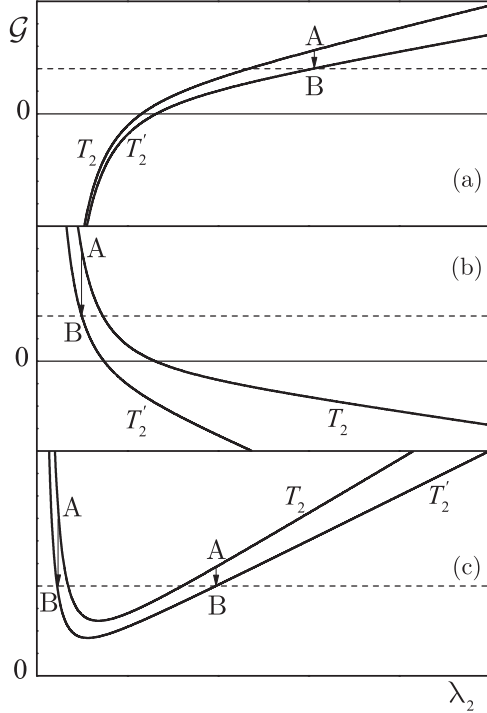


FIG. 2. Typical dependence of the reduced torque \mathcal{G} on stretch λ_2 corresponding to cases (a)–(c) in the main text. The reduced external torques $G_{\text{ext}}/\mu A_0 R_1$ are represented by the dashed lines.

(d) If $P_{\parallel} - \gamma < 0$ and $P_{\perp} - 1/\gamma^2 > 0$, then $\mathcal{G} < 0$; there are no solutions for $G_{\text{ext}} > 0$. Reversing the external torque, and cooling rather than heating to T_2 , reverses the motor and we have an analogy to case (c).

We adopt a simple freely jointed rod model for the polymer backbones, with a step length a in the isotropic state. Then the step lengths are $\ell_{\parallel} = a(1 + 2Q)$ and $\ell_{\perp} = a(1 - Q)$, with the nematic order parameter $0 \leq Q \leq 1$. Although crude, this model quite accurately describes a wide range of LCEs [1, 10], and, in particular, the development of photoforce [11].

The material parameters P_{\parallel} and P_{\perp} now read $P_{\parallel} = (1 + 2Q_1)/(1 + 2Q_2)$ and $P_{\perp} = (1 - Q_1)/(1 - Q_2)$, where $Q_1 = Q(T_1)$ and $Q_2 = Q(T_2)$. Then the above material conditions can be expressed in terms of Q_1 and Q_2 . For example, the condition $P_{\parallel} > 1/\sqrt{P_{\perp}}$ of case (a) is $g(Q_1) > g(Q_2)$, where $g(Q) = 3Q - 4Q^3$. Since $Q_1 > Q_2$, the condition $g(Q_1) > g(Q_2)$ is satisfied whenever $Q_1 \leq 1/2$. Further, for every Q_1 lying in the interval $1/2 < Q_1 < \sqrt{3}/2$, one can find a threshold value of Q_2 below which the condition $g(Q_1) > g(Q_2)$ holds. Lastly, for $Q_1 \geq \sqrt{3}/2$ the condition $g(Q_1) > g(Q_2)$ cannot be satisfied. The material condition $P_{\parallel} < 1/\sqrt{P_{\perp}}$ of (b) is $g(Q_1) < g(Q_2)$, and corresponding conditions in terms of Q are easily obtained. In case (c) one has $\gamma < \min(P_{\parallel}, 1/\sqrt{P_{\perp}})$. If the temperature T_2 is above the nematic-isotropic transition temperature, one has $Q_2 = 0$, and consequently $P_{\parallel} > 1/\sqrt{P_{\perp}}$ for all $Q_1 < \sqrt{3}/2$.

We estimate the efficiency of the engine as $\eta = P_{\text{out}}/P_{\text{in}}$, where P_{in} is the power needed to heat an incoming element of the elastomer at temperature T_1 to temperature T_2 , and P_{out} is the corresponding power output. The input power can be expressed as $P_{\text{in}} = C_p \Delta T A_0 (dl_0/dt)$, where dl_0 is the length

of a piece of the elastomer in the formation state, currently stretched by λ_1 . Here C_p denotes the isobaric heat capacity per unit volume of the elastomer and $\Delta T = T_2 - T_1$. For an element of the elastomer lying on the wheel of radius R_2 , one can write $\lambda_1 (dl_0/dt) = \omega R_2$, where ω is the angular velocity. The output power is $P_{\text{out}} = G_{\text{ext}} \omega$. The reduced efficiency, $\tilde{\eta} = \eta C_p \Delta T / \mu$, arises through Eq. (8) and is

$$\tilde{\eta} = (\gamma - 1) \left[\lambda_2^2 (P_{\parallel} - \gamma) - \left(P_{\perp} - \frac{1}{\gamma^2} \right) \frac{1}{\lambda_2} \right], \quad (9)$$

where λ_2 is given by Eq. (3).

We roughly estimate $C_p \Delta T$ using the latent heat per unit volume of an idealized, sharp (first-order) nematic-isotropic transition. Its approximate value is $2 \times 10^6 \text{ J m}^{-3}$ [1]. Since the isotropic shear modulus is of the order $\mu \sim 10^5 - 10^6 \text{ J m}^{-3}$, then $\mu/C_p \Delta T$ can be up to 0.5. For photoelastomers the energy input $C_p \Delta T$ represents $\varepsilon n_{\text{dye}}$, where ε is the photon energy and n_{dye} is the number density of dye molecules [12], giving for $\mu/\varepsilon n_{\text{dye}}$ an estimate of the same order as that for $\mu/C_p \Delta T$.

As we have seen, when $Q_2 = 0$, the constraint is $P_{\parallel} > 1/\sqrt{P_{\perp}}$, which restricts us to cases (a) or (c). The efficiency (9) depends on four dimensionless quantities: the order parameter Q_1 (through $P_{\parallel} = 1 + 2Q_1$ and $P_{\perp} = 1 - Q_1$), the reduced lengths \tilde{L} and \tilde{L}_0 (through λ_2), and the ratio of the wheel radii γ . Clearly, the efficiency increases with increasing order Q_1 . Regarding the efficiency as a function of \tilde{L}_0 , $\tilde{\eta}$ takes quite large values for $\tilde{L}_0 \ll 1$ as well as for $\tilde{L}_0 \gg 1$. Similarly, the efficiency increases with increasing \tilde{L} . The engine can operate only if certain physical constraints are satisfied, implying that \tilde{L}_0 and \tilde{L} are not completely independent of each other. First, to obtain a contractile force, the stretch λ_2 should be greater than the natural contraction λ_m of the freely suspended elastomer, which can be expressed as $\gamma < \tilde{L}/(\tilde{L}_0 \lambda_m - \tilde{L} - 2)$. This condition, together with $\gamma > 1$, implies that $\tilde{L}_0 \lambda_m / 2 - 1 < \tilde{L} < \tilde{L}_0 \lambda_m - 2$. Besides, since one

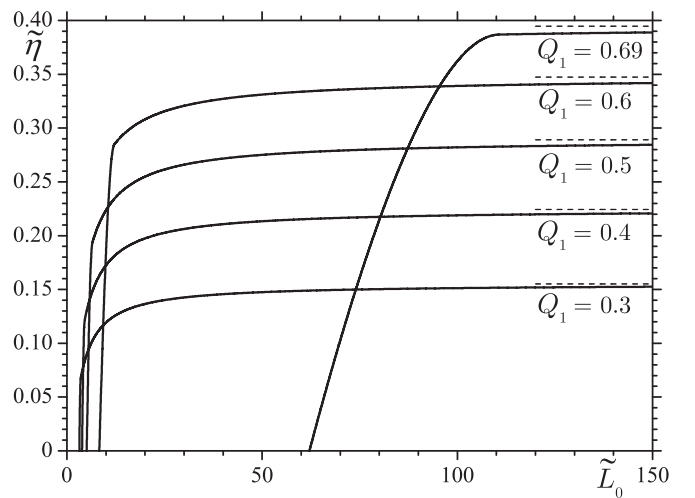


FIG. 3. The reduced efficiency $\tilde{\eta}$ as a function of \tilde{L}_0 for different values of Q_1 (solid lines). Along the plateau of each of these curves the optimal values of γ change only slightly, taking the values $\gamma \approx 1.22, 1.28, 1.34, 1.40, 1.47$ for $Q_1 = 0.3, 0.4, 0.5, 0.6, 0.69$, respectively. The dashed lines correspond to $\tilde{L}_0 \gg 1$. The efficiency $\eta = \tilde{\eta} \mu / (\varepsilon n_{\text{dye}})$ can go up to 20%.

cannot mechanically contract a thin elastomer below its natural length, then $\lambda_1 > 1$. The ratio γ is thus limited from below, $\gamma > (\tilde{L}_0 - \tilde{L})/(\tilde{L} + 2)$. In addition, to avoid slack when the elastomer is stretched from its formation state and wound around the pulleys, one has $\gamma > \tilde{L}_0 - 2\tilde{L} - 1$. In summary,

$$\gamma > \max\left(1, \frac{\tilde{L}_0 - \tilde{L}}{\tilde{L} + 2}, \tilde{L}_0 - 2\tilde{L} - 1\right),$$

$$\gamma < \min\left(P_{\parallel}, \frac{\tilde{L}}{\tilde{L}_0\lambda_m - \tilde{L} - 2}\right),$$
(10)

taking into account that $\gamma < P_{\parallel}$, a consequence of the reasonable assumption $Q_1 < \sqrt{3}/2$.

The optimal value of $\tilde{\eta}$ is obtained by choosing \tilde{L} as large as possible, $\tilde{L} = \tilde{L}_0\lambda_m - 2$, then maximizing $\tilde{\eta}$ with respect to γ and making sure that the constraints (10) are satisfied. Numerical results for the reduced efficiency $\tilde{\eta}$ are shown in Fig. 3. Optimal values of $\tilde{\eta}$ are reached already for moderate $\tilde{L}_0 \approx 20$ for $Q_1 \lesssim 0.6$. The efficiency $\eta = \tilde{\eta}\mu/(\epsilon n_{\text{dye}})$ can go up to 20% for $Q_1 \approx 0.7$ in the optical case. For $Q_1 > 0.7$, the no slack condition (10) is violated. Such high values of

Q_1 in Fig. 3 are perhaps unphysical in side-chain LCEs, but they represent the high anisotropy in P_{\parallel} and P_{\perp} found in main-chain elastomers serving as working materials. Their P_{\parallel} and P_{\perp} values are more extreme, even at normal values of Q_1 , and $1/\lambda_m$ can be as large as 350% [4]. For photoengines, the thickness of the elastomer band depends critically on the light intensity. Nonlinear absorption processes determine optical penetration and force dynamics [11,12]; for mm thicknesses intensities of 10–100 mW/cm² are required—smaller than maximal insolation.

In summary, the thermo-optical contraction of nematic elastomers can be used to harness thermal or optical energy to generate mechanical energy. Further efficiency can be gained in both material design and geometric improvements to the engine.

M.K. acknowledges support from the Winton Programme for the Physics of Sustainability and the Cambridge Overseas Trust, and M.W. thanks the Engineering and Physical Sciences Research Council (UK) for support through a Senior Fellowship. We are grateful to E. M. Terentjev and P. Palfy-Muhoray for useful discussions.

-
- [1] M. Warner and E. M. Terentjev, *Liquid Crystal Elastomers* (Oxford University Press, Oxford, UK, 2007).
 - [2] P. G. de Gennes, C. R. Seances Acad. Sci., Ser. B **281**, 101 (1975).
 - [3] H. Finkelmann and H. Wermter, Abstr. Pap. Am. Chem. Soc. **219**, 189 (2000).
 - [4] A. R. Tajbakhsh and E. M. Terentjev, *Eur. Phys. J. E* **6**, 181 (2001).
 - [5] H. Finkelmann, E. Nishikawa, G. G. Pereira, and M. Warner, *Phys. Rev. Lett.* **87**, 015501 (2001).
 - [6] P. M. Hogan, A. R. Tajbakhsh, and E. M. Terentjev, *Phys. Rev. E* **65**, 041720 (2002).
 - [7] I. Z. Steinberg, A. Oplatka, and A. Katchalsky, *Nature (London)* **210**, 568 (1966).
 - [8] M. Yamada, M. Kondo, J. Mamiya, Y. Yu, M. Kinoshita, C. J. Barrett, and T. Ikeda, *Angew. Chem. Int. Ed.* **47**, 4986 (2008).
 - [9] Y. Geng, P. L. Almeida, S. N. Fernandes, C. Cheng, P. Palfy-Muhoray, and M. H. Godinho, *Sci. Rep.* **3**, 1028 (2013).
 - [10] H. Finkelmann, A. Greve, and M. Warner, *Eur. Phys. J. E* **5**, 281 (2001).
 - [11] M. Knežević, M. Warner, M. Čopič, and A. Sánchez-Ferrer, *Phys. Rev. E* **87**, 062503 (2013).
 - [12] M. Knežević and M. Warner, *Appl. Phys. Lett.* **102**, 043902 (2013).